

## Comparative Crystal Chemistry of Spinels from Some Suites of Ultramafic Rocks

F. Princivalle<sup>1</sup>, A. Della Giusta<sup>2</sup>, and S. Carbonin<sup>2</sup>

<sup>1</sup>Istituto di Mineralogia e Petrografia, Università di Trieste, and

<sup>2</sup>Dipartimento di Mineralogia e Petrologia, Università di Padova, Italy

With 3 Figures

Received May 24, 1988;

accepted February 9, 1989

### Summary

Microprobe analyses and X-ray crystal structure refinement data of Mg–Fe–Al–Cr spinels from different environments are compared. The investigated crystals represent both restitic and recrystallized spinels from an Alpine peridotitic massif, and restitic spinels from four suites of ultramafic xenoliths. Within each suite the crystals represent different steps of an increasing melting process, which causes a strong increase in Cr<sup>3+</sup> and a moderate increase in Fe<sup>2+</sup>, with depletion of Al<sup>3+</sup> and Mg<sup>2+</sup>. Within each suite, in spite of relevant bulk chemistry changes, the ratio of the octahedral to tetrahedral coordination distances, and consequently the oxygen positional parameter  $x$ , are kept constant. Conversely,  $x$  may differ in suites with similar bulk chemistry, mainly due to different Mg–Al ordering between octahedral and tetrahedral sites. This suggests that the  $x$  parameter is strongly affected by physical environment, and that consequently, within the range of the investigated compositions, it could be used as a marker.

### Zusammenfassung

*Vergleich der Kristallchemie von Spinellen aus einigen Suiten von ultramafischen Gesteinen*

EMS-Analyse und röntgenografisch verfeinerte Kristallstrukturen von Mg–Fe–Al–Cr Spinellen aus verschiedenen petrologischen Situationen wurden verglichen. Unter den untersuchten Kristallen befinden sich sowohl restitische und rekristallisierte Spinelle aus alpinen Peridotiten, als auch restitische Spinelle aus vier Suiten von ultramafischen Xenolithen. Die Kristalle in jeder Suite gehören zu verschiedenen Stufen eines Schmelzprozesses, der ein starkes Anwachsen der Cr<sup>3+</sup>- und ein mäßiges Anwachsen der Fe<sup>2+</sup>-Konzentration bei gleichzeitiger Verminderung des Al<sup>3+</sup>- und Mg<sup>2+</sup>-Gehaltes, verursacht. Jede Suite zeigt, trotz bedeutender chemischer Veränderungen, ein feststehendes Verhältnis von oktaedrischen zu tetraedrischen Polyederdimensionen, weshalb

der Sauerstoffparameter  $x$  unveränderlich bleibt. Jedoch sehen wir, daß sich die  $x$  von den Spinellen zweier verschiedener Suiten mit ähnlichem Chemismus unterscheiden, was auf die unterschiedliche Mg-Al-Anordnung in oktaedrischen und tetraedrischen Positionen zurückzuführen ist. Dies läßt vermuten, daß der Parameter  $x$  sehr stark von der petrogenetischen Situation abhängig ist, was bedeutet, daß er als Anhaltspunkt zum Verständnis der physikalischen Entstehungsbedingungen verwendet werden kann.

## Introduction

Work on the crystal chemistry of spinels of mantle origin (*Della Giusta et al.*, 1986) has recently revealed that the oxygen atomic coordinate in the structure of these minerals maintains an essentially constant value, in spite of the substantial bulk chemistry changes involved. In a previous paper, *Basso et al.* (1984) studied the crystal chemistry of spinels with similar bulk chemistry but from different geodynamic environments; other crystal chemical data of spinels have recently become available from a suite of spinel lherzolite xenoliths (*Cundari et al.*, 1986). In the two latter cases, it appears that the oxygen atomic coordinate is rather constant within a well-defined petrogenetic process; conversely, it varies if spinels of different origin are compared. In order to clarify the possible relations between this spinel structural parameter and the particular environment of formation, we investigated the crystal chemistry of more spinels which, as in the previous examples, were well defined as to their origin. We also supplied already studied series with new crystal chemical data. This paper presents new results on the crystal chemistry of Mg-Al-Fe-Cr spinels in peridotitic rocks from Assab, Ethiopia, and North-Eastern Brazil, together with new contributions from Balmuccia, Western Italian Alps, and Mt. Noorat, Australia. All these results are compared with the already published data from Mts. Leura and Noorat, and from the Balmuccia peridotite. The suites to which the spinels belong consist of mantle nodules of lherzolite to harzburgite composition. The Balmuccia suite is a peridotite massif, and the investigated crystals represent both restitic (TS28, TS32) and recrystallized spinels from veins trapped within it (*Sinigoï et al.*, 1983). In all cases partial melting of the host rock caused a strong depletion of clinopyroxene, followed by a relevant increase of the Cr content and a decrease of the Mg/Fe ratio in spinel, relative to the other coexisting phases (orthopyroxene, clinopyroxene and olivine). For detailed petrological information the reader is referred to: Mts. Leura and Noorat (Australia): *Irving* (1974), *Frey and Green* (1974), *Ellis* (1976); Assab (Ethiopia): *Piccardo et al.* (1978), *Otonello et al.* (1978a, 1978b, 1980); North-Eastern Brazil: *Comin-Chiaramonti et al.* (1986); Balmuccia (Western Italian Alps): *Sinigoï et al.* (1983). Crystal chemical investigations on coexisting phases in some of the above-mentioned series have already been performed on: olivine from Mt. Leura and Assab by *Princivalle and Secco* (1985) and *Basso et al.* (1979) respectively; clino- and orthopyroxene from Mts. Leura and Noorat by *Dal Negro et al.* (1984), *Cundari et al.* (1986), *Secco* (1988); and clinopyroxene from North-Eastern Brazil by *Princivalle et al.* (1989).

## Experimental

The analyzed crystals were selected from rock sections about 100  $\mu\text{m}$  thick by use of a petrographic microscope. X-ray intensities were measured by a SIEMENS AED

II four-circle diffractometer up to 50–55 degrees  $\theta$ , using Mo monochromatized radiation and omega scan mode, with peak-base widths of  $2^\circ 2\theta$ , 45-step integration and 0.6 second counting time per step. Six equivalent reflections were measured and corrected for absorption and background according to *North et al. (1968)* and *Blessing et al. (1972)*. The data were corrected for Lorentz and polarization effects and isotropic secondary extinction. No reflection inconsistent with  $Fd3m$  symmetry was detected. 22 accurately centred reflections were used for cell parameter determination. Scattering curves for 50% ionized atoms were used, since they led to the best agreement in the low  $\sin \theta/\lambda$  range. The results of structure refinement, performed with STRUCSY programs (STOE copyright), are shown in Table 1. The same crystals used for X-ray data collection were mounted on glass slides and polished for electron microprobe analysis. This was carried out on an energy-dispersive microprobe (ETEC Autoscan SEM and ORTEC EEDS spectrometer) operating at 15 KV, 10  $\mu$ A. A Magic Program (*Colby, 1972*) in the ORTEC MAGIC IV M version was used to convert X-ray counts into weight % of oxides. Three to six analyses were obtained from each crystal, showing good chemical homogeneity. The analytical results are given in Table 2. In order to define the accuracy of our results and thus more effectively interpret the meaning of our data, two crystals of spinels from Mt. Leura, LE7 and LE8, the same as those studied by *Della Giusta et al. (1986)*, were analyzed by means of wavelength-dispersive fully automated ARL-SEM-Q instruments in the Universities of Milan and Modena and also by means of a JXA-5A system in the University of Melbourne. The maximum variations found among the various instruments are shown in Fig. 2 as vertical bars indicating atomic proportions for major cations. Columns with an asterisk in Tables 1 and 2 refer to data partly published by *Basso et al. (1984)*, reported here for ease of comparison, since all the cation distributions were recalculated with the method and the bond distances used by *Della Giusta et al. (1986)*. Original sample numbers are quoted in the tables; reference to the last two digits only is made in the figures.

### Crystal Structure Considerations

In spinels, the anions form a nearly cubic close-packed array, parallel to (111) planes, and the cations fill part of the tetrahedral (T) and octahedral (M) interstices available in the framework. The oxygen atom is linked to three octahedral and one tetrahedral cations, lying respectively on opposite sides of the oxygen layer, to form a trigonal pyramid. The fractional coordinates of the only oxygen atom in the unit cell (point symmetry  $3m$  in space group  $Fd3m$ , origin at  $\bar{3}m$ ) are  $(x, x, x)$  and may assume values ranging from 0.239 (if the origin is chosen at  $\bar{3}m$ ) in  $\text{MoAg}_2\text{O}_4$  to 0.269 in  $\text{CdV}_2\text{O}_4$  (*Hill et al., 1979*). If these values were exactly equal to 0.25, an ideal cubic close-packed structure would result and the coordination polyhedra, the T and M sites, would both be ideal, with all edges equal to each other. Deviation from this value (i.e. movement of the oxygen atom along the cube diagonal  $[111]$ ) causes the oxygen layers in the spinel structure to be slightly puckered (*Lindsley, 1976*) so that only the tetrahedron remains regular (point symmetry  $\bar{4}3m$ , coordinates  $1/8, 1/8, 1/8$ ), whereas the octahedron lowers its symmetry to  $\bar{3}m$  (coordinates  $1/2, 1/2, 1/2$ ), its angles and edges no longer being equal to each other (Table 1). *Hafner (1970, Fig. 1)* highlighted the role played by the oxygen parameter  $x$  on the deformation of the octahedral site along the direction of the 3-fold axis. Only the position of the

Table 1. Cell edge and selected crystal structure refinement data in spinels. B eq. = isotropic temperature factor equivalent to anisotropic values. Columns with asterisks: data by Basso et al. (1984). Occ. Mg(T) vs Fe and Al(M) vs Cr (except for TS2 and TS25: Al(M) vs Fe; Basso et al., 1984). No. rifl. = number of observed reflections used for refinement.

$$R = \frac{\sum ||F_{obs}| - |F_{calc}||}{\sum |F_{obs}|}$$

Sample	NORTH-EASTERN BRAZIL										ASSAB (ETHIOPIA)				
	CC 37	SA 24	CC 29	CC 34	3G 12	3G 15	3G 51	3G 18							
a <sub>0</sub> (Å)	8.1384 (4)	8.1402 (5)	8.1810 (5)	8.2402 (5)	8.1521 (10)	8.1777 (17)	8.2258 (7)	8.2298 (11)							
x	0.2626 (1)	0.2626 (1)	0.2624 (2)	0.2625 (2)	0.39	0.45	0.52	0.44							
B eq. (T)	0.65	0.60	0.65	0.65	0.28	0.32	0.39	0.31							
B eq. (M)	0.55	0.44	0.53	0.49	0.53	0.61	0.65	0.49							
B eq. (O)	0.80	0.72	0.79	0.75	0.771 (6)	0.725 (7)	0.717 (15)	0.717 (15)							
occ. Mg (T)	0.793 (15)	0.785 (17)	0.764 (22)	0.696 (18)	0.762 (9)	0.707 (11)	0.541 (19)	0.484 (22)							
occ. Al (M)	0.889 (23)	0.884 (24)	0.723 (39)	0.485 (36)	1.945 (2)	1.949 (2)	1.960 (2)	1.961 (2)							
T-O	1.940 (2)	1.940 (2)	1.947 (3)	1.962 (3)	1.939 (3)	1.947 (2)	1.958 (2)	1.959 (3)							
M-O	1.937 (2)	1.938 (2)	1.949 (4)	1.962 (4)	0.9967	0.9989	0.9989	0.9989							
M-O/T-O	0.9989	1.0011	1.0000	1.0000	3.177	3.183	3.201	3.203							
tet. edge	3.167	3.168	3.179	3.205	2.587	2.600	2.615	2.616							
oct. edge (a)	2.587	2.588	2.605	2.622	2.890	2.899	2.916	2.917							
oct. edge (b)	2.885	2.885	2.900	2.921	194	208	134	206							
No. rifl.	121	133	100	99	0.013	0.015	0.018	0.024							
R	0.031	0.028	0.027	0.023											

Sample	BALMUCCIA (ITALIAN WESTERN ALPS)					MT. NOORAT (AUSTRALIA)					
	TS 2	TS 25	TS 11	TS 28B	TS 32	R. 28181	R. 28188	R. 28187			
a <sub>0</sub> (Å)	8.1140 (30)	8.1110 (30)	8.1220 (30)	8.1320 (30)	8.1944 (4)	8.1466 (3)	8.1638 (3)	8.2346 (4)			
x	0.2635 (1)	0.2638 (1)	0.2638 (1)	0.2637 (1)	0.2634 (1)	0.2626 (1)	0.2624 (1)	0.2625 (1)			
B eq. (T)	0.42	0.40	0.35	0.38	0.65	0.67	0.56	0.64			
B eq. (M)	0.35	0.35	0.30	0.30	0.51	0.54	0.49	0.44			
B eq. (O)	0.38	0.31	0.28	0.33	0.72	0.77	0.73	0.65			
occ. Mg (T)	0.782 (1)	0.756 (1)	0.736 (1)	0.720 (1)	0.660 (10)	0.780 (20)	0.800 (10)	0.710 (10)			
occ. Al (M)	0.971 (2)	0.961 (2)	0.925 (1)	0.841 (1)	0.710 (10)	0.830 (30)	0.770 (10)	0.520 (20)			
T-O	1.946 (2)	1.950 (2)	1.953 (2)	1.954 (2)	1.964 (2)	1.942 (2)	1.943 (2)	1.961 (2)			
M-O	1.925 (2)	1.922 (2)	1.925 (2)	1.928 (2)	1.945 (2)	1.939 (2)	1.945 (2)	1.961 (2)			
M-O/T-O	0.9891	0.9858	0.9858	0.9869	0.9902	0.9989	1.0011	1.0000			
tet. edge	3.179	3.184	3.189	3.190	3.208	3.171	3.173	3.203			
oct. edge (a)	2.559	2.551	2.555	2.560	2.587	2.590	2.600	2.620			
oct. edge (b)	2.877	2.876	2.880	2.884	2.905	2.888	2.893	2.919			
No. rifl.	93	94	96	95	149	147	145	173			
R	0.022	0.025	0.018	0.021	0.029	0.039	0.039	0.038			

(a): shared octahedral edge; (b): unshared octahedral edge

Table 2. Microprobe analyses and cation distribution in T and M sites (per 4 oxygens), the latter resulting from minimization process (see text). Columns with asterisks: data published by Basso et al. (1984), recalculated on basis of bond distances used in this work

Sample	NORTH-EASTERN BRAZIL				ASSAB (ETHIOPIA)			
	CC 37	SA 24	CC 29	CC 34	3G 12	3G 15	3G 51	3G 18
MgO	21.44	21.25	19.87	16.96	19.79	18.10	17.08	16.31
Al <sub>2</sub> O <sub>3</sub>	57.86	56.71	45.00	28.71	48.53	42.53	33.28	28.27
FeO <sub>t</sub>	10.71	9.99	12.13	14.97	11.79	14.03	14.45	15.10
Cr <sub>2</sub> O <sub>3</sub>	10.09	12.15	22.62	38.57	19.80	24.98	34.84	39.98
NiO	0.34	0.29	0.23	0.14	0.26	0.21	0.16	0.10
MnO	0.08	0.13	0.11	0.14	0.08	0.14	0.18	0.17
TiO <sub>2</sub>	0.09	0.04	0.11	0.02	0.08	0.24	0.04	0.04
SiO <sub>2</sub>	0.13	0.10	0.05	0.11	0.12	0.08	0.05	0.06
Sum	100.74	100.66	100.12	99.62	100.45	100.31	100.08	100.03
T site:								
Mg	0.649	0.640	0.656	0.652	0.664	0.641	0.651	0.646
Al	0.151	0.150	0.118	0.052	0.114	0.085	0.067	0.055
Fe <sup>2+</sup>	0.184	0.187	0.195	0.262	0.199	0.208	0.257	0.281
Fe <sup>3+</sup>	0.011	0.018	0.028	0.027	0.018	0.061	0.020	0.012
Mn	0.002	0.003	0.002	0.004	0.002	0.003	0.004	0.004
Si	0.003	0.002	0.001	0.003	0.003	0.002	0.001	0.002
Sum	1.000	1.000	1.000	1.000	1.000	1.000	1.000	1.000
M site:								
Al	1.586	1.565	1.313	0.938	1.408	1.292	1.056	0.925
Cr	0.204	0.246	0.484	0.893	0.417	0.543	0.791	0.926
Mg	0.168	0.173	0.145	0.088	0.122	0.101	0.079	0.068
Fe <sup>2+</sup>	0.002	0.000	0.009	0.005	0.009	0.049	0.017	0.001
Fe <sup>3+</sup>	0.031	0.009	0.042	0.073	0.036	0.005	0.053	0.077
Ni	0.007	0.006	0.005	0.003	0.006	0.005	0.003	0.002
Ti	0.002	0.001	0.002	0.000	0.002	0.005	0.001	0.001
Sum	2.000	2.000	2.000	2.000	2.000	2.000	2.000	2.000
Cr/R <sup>3+</sup>	0.103	0.124	0.244	0.450	0.209	0.273	0.398	0.464
-----								
Sample	BALMUCCIA (ITALIAN WESTERN ALPS)				Mt. NOORAT (AUSTRALIA)			
	* TS 2	* TS 25	* TS 11	* TS 28B	TS 32	R.28181	R.28188	R.28187
MgO	20.55	21.24	19.71	19.77	15.18	20.53	19.71	16.70
Al <sub>2</sub> O <sub>3</sub>	64.45	64.85	61.00	55.36	41.00	52.08	48.19	29.27
FeO <sub>t</sub>	13.55	12.24	14.48	13.47	17.22	10.10	11.46	14.18
Cr <sub>2</sub> O <sub>3</sub>	0.87	1.01	4.25	10.47	26.13	14.75	20.05	39.22
NiO	0.00	0.23	0.30	0.31	0.19	0.37	0.32	0.21
MnO	0.18	0.14	0.13	0.17	0.13	0.07	0.10	0.19
TiO <sub>2</sub>	0.03	0.00	0.00	0.04	0.15	0.11	0.13	0.24
SiO <sub>2</sub>	0.06	0.00	0.00	0.05	0.00	0.03	0.03	0.00
Sum	99.69	99.71	99.87	99.64	100.00	98.04	99.99	100.01
T site:								
Mg	0.692	0.691	0.682	0.698	0.593	0.662	0.650	0.647
Al	0.089	0.080	0.056	0.040	0.057	0.127	0.151	0.062
Fe <sup>2+</sup>	0.158	0.178	0.191	0.180	0.326	0.172	0.196	0.258
Fe <sup>3+</sup>	0.056	0.048	0.068	0.078	0.021	0.036	0.000	0.029
Mn	0.004	0.003	0.003	0.003	0.003	0.002	0.002	0.004
Si	0.001	0.000	0.000	0.001	0.000	0.001	0.001	0.000
Sum	1.000	1.000	1.000	1.000	1.000	1.000	1.000	1.000
M site:								
Al	1.829	1.840	1.787	1.664	1.290	1.507	1.367	0.945
Cr	0.017	0.020	0.086	0.217	0.575	0.311	0.424	0.904
Mg	0.082	0.104	0.070	0.073	0.061	0.154	0.138	0.081
Fe <sup>2+</sup>	0.070	0.022	0.050	0.037	0.020	0.010	0.013	0.017
Fe <sup>3+</sup>	0.001	0.010	0.001	0.001	0.047	0.008	0.048	0.043
Ni	0.000	0.004	0.006	0.007	0.004	0.008	0.007	0.005
Ti	0.001	0.000	0.000	0.001	0.003	0.002	0.003	0.005
Sum	2.000	2.000	2.000	2.000	2.000	2.000	2.000	2.000
Cr/R <sup>3+</sup>	0.009	0.010	0.043	0.108	0.289	0.156	0.213	0.455
-----								
FeO <sub>t</sub>	as total iron							

oxygen atom and the value of the cell dimension may vary within the structure, whereas the tetrahedral and octahedral cations are fixed in special positions. Simple exact relations (Hill et al., 1979) exist between the two independent geometric parameters (oxygen coordinate  $x$  and cell dimension  $a_0$ ) and the cation-anion tetrahedral and octahedral distances, (T-O) and (M-O). These relations show that  $a_0$  is an increasing function with (T-O) and (M-O), while  $x$ , the oxygen coordinate, depends only on the ratio (M-O)/(T-O). The relations between (M-O) and (T-O) and the oxygen coordinate were also enhanced by Hafner (1970, Fig. 2): with increasing  $x$ , (M-O)/ $a_0$  decreases while (T-O)/ $a_0$  increases. For  $x < 0.2625$ , (M-O) is greater than (T-O), and vice versa for  $x > 0.2625$ .

We may take the value of  $x = 0.2625$  as a reference point to discuss the changes occurring in our samples.

### Discussion

In Tables 1 and 2 the samples are ordered according to increasing Cr content, which leads to a strong increase in the  $a_0$  cell edge. It is interesting to note that all the

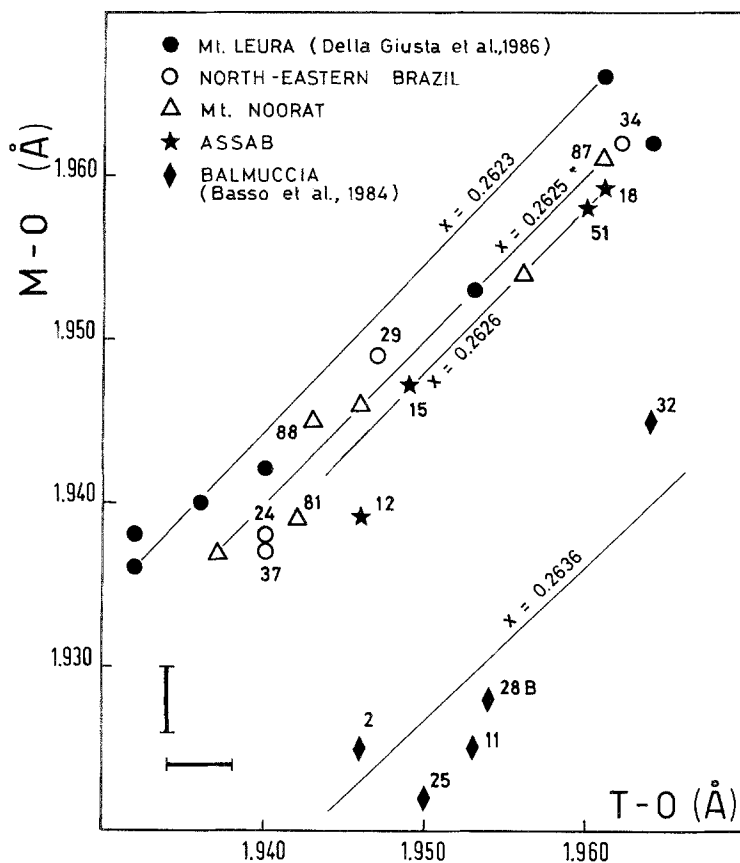


Fig. 1. Variation of (T-O) vs (M-O) bond distances in spinels. New data from Mt. Noorat indicated by sample numbers, old data after Cundari et al. (1986), reported by symbols only. Old and new data from Balmuccia (see Table 2) indicated in detail. Straight lines drawn using  $x$  mean of each series (see text). Error bars: mean standard deviations relative to (T-O) and (M-O)

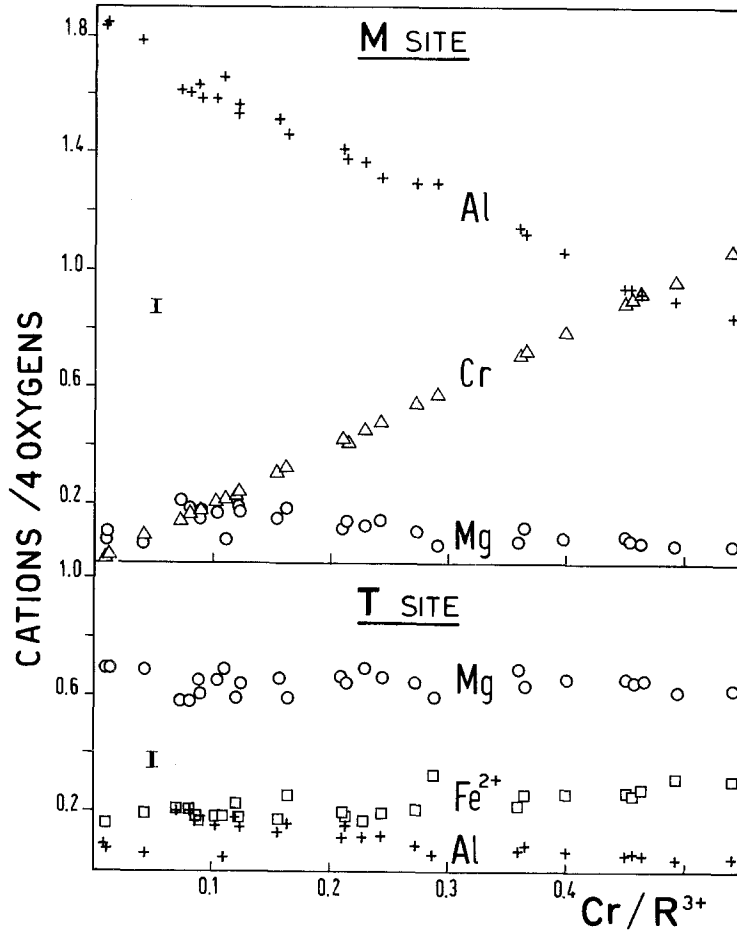


Fig. 2. Variation of major cations in M and T sites in all series, plotted against  $\text{Cr}/\text{R}^{3+}$ . ( $\text{R}^{3+} = \text{Al} + \text{Fe}^{3+} + \text{Cr}$ ). Error bars: maximum variations found in cation proportions, after test analyses performed on the same crystals with different instruments (see text)

samples belonging to the same suite have approximately the same oxygen parameter  $x$ . The Mt. Leura spinels, having a mean value of 0.2623 (1), have (M-O) distances which are always greater than (T-O). The North-Eastern Brazil and Mt. Noorat samples, both with  $x = 0.2625(1)$ , have (M-O) very close or equal to (T-O). The Assab samples, with  $x = 0.2626(1)$ , have (M-O) a little shorter than (T-O). Lastly, the Balmuccia samples, with  $x = 0.2636(2)$ , have (M-O) a great deal shorter than (T-O). The relations between (M-O) and (T-O) are plotted in Fig. 1. Let us see how the  $x$  parameter, and consequently the (M-O)/(T-O) ratio, can be constant within a suite in spite of relevant chemical changes, while it may differ between samples of similar bulk chemistry but belonging to different suites. In discussing our data we shall: 1) consider the changes within a single suite as  $\text{Cr}/\text{R}^{3+}$  increases with increasing degrees of partial melting, and 2) examine the differences between suites with similar bulk chemistry.

1) With increasing degree of melting, the relevant substitutions occurring in the spinel structure are: Cr enters the M site at the expense of both  $\text{Al}^{3+}$  (Fig. 2) and

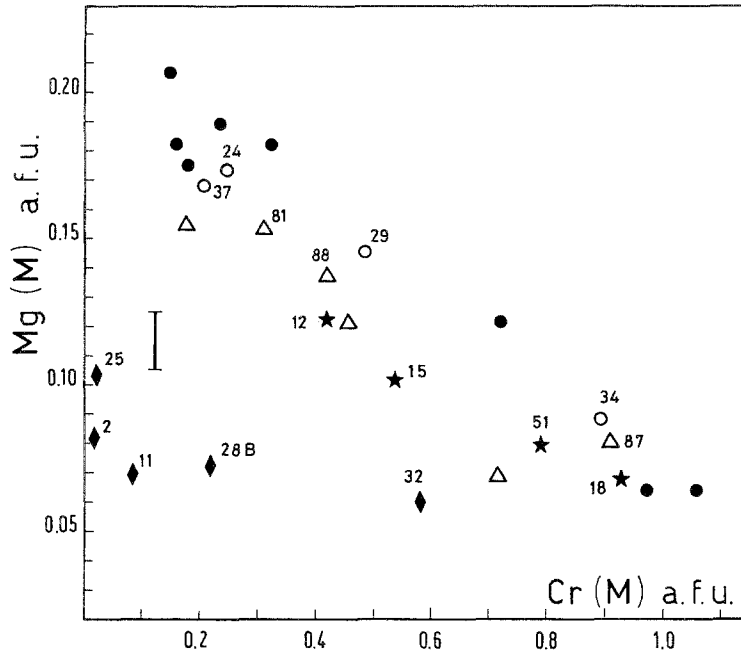


Fig. 3. Mg(M) vs Cr(M) (*a.f.u.* = atoms per formula unit). Symbols as in Fig. 1. Error bar: maximum error estimated for Mg(M). In spite of relatively high uncertainty in evaluation of Mg(M) atomic proportion and therefore of scattering of representative points, differences among the series are noticeable and recall trends in Fig. 1

Mg<sup>2+</sup> (Fig. 3), causing a lengthening of the (M-O) distance, while Fe<sup>2+</sup> substitutes for Al<sup>3+</sup> in the T site, similarly increasing the (T-O) distance. Therefore, Cr<sup>3+</sup> and Fe<sup>2+</sup> cause a concomitant increase in the sizes of M and T sites, so that (M-O)/(T-O) and consequently  $x$  are kept constant, as shown in Fig. 1.

2) Spinels with similar bulk chemistry, but belonging to different suites exhibit a wide range of  $x$  values, from 0.2623 (Mt Leura) to 0.2636 (Balmuccia). This depends on differences in the cation distribution among different suites. Cr<sup>3+</sup> can only be assigned to the M site on the basis of its strong octahedral preference (*O'Neill and Navrotsky, 1983, Urusov, 1983*); Fe<sup>2+</sup> shows a systematic ordering in the T site (Table 2); other cations (Fe<sup>3+</sup>, Mn<sup>2+</sup>, Si, Ni and Ti) occur in lesser quantities and so do not significantly influence the sizes of the sites. Mg<sup>2+</sup> and Al<sup>3+</sup> are the only cations present in relevant amounts in both T and M sites; the differences in their distribution are responsible for the  $x$  differences among different suites. For similar Cr content, crystals with relevant amounts of Al<sup>3+</sup> (T) and Mg<sup>2+</sup> (M), e.g. Mt. Leura, have shorter (T-O) and longer (M-O) distances and, consequently, lower values of  $x$  (Fig. 1). These differences are evident in Fig. 3, showing in more detail than Fig. 2 how Mg(M) decreases with increasing Cr<sup>3+</sup> in different suites. It is evident that—for similar Cr content—each suite has different Mg(M) and hence different Mg–Al distribution (see Table 2). We can also see from Fig. 3 that, at the end of the partial melting process, all the suites reach an almost equal minimum value of Mg(M) = 0.06 a.f.u., corresponding to very different Cr<sup>3+</sup> values; these range from 0.57 a.f.u. for Balmuccia to 1.06 a.f.u. for Mt. Leura, the higher values corresponding to the suites with lower  $x$  oxygen coordinate.



## Conclusions

The spinel  $x$  oxygen coordinate seems to be a discriminant parameter among the investigated suites. The  $x$  differences depend mainly on different distributions of Mg and Al between tetrahedral and octahedral sites. Its almost constant value inside a single suite is not related to relevant bulk chemistry changes occurring within the suite. It is worth observing that  $x$  keeps an almost constant value even in a suite like Balmuccia, which includes both restitic and recrystallized spinels. The very slow cooling of the Balmuccia peridotite is associated with highly ordered Mg–Al distribution in spinel, with Mg essentially in the T and Al in the M sites, contrary to the relevant disorder in the nodule spinels of the remaining suites that suffered rapid quenching from high temperatures. The different distribution of Mg and Al between the two sites, typical of each suite, may testify to the different temperature at which the exchange between the two ions ceased inside the crystal. This suggests that the cation distribution and consequently the  $x$  are to some extent determined by the cooling history of these phases in the rocks.

## Acknowledgements

Giulio Ottonello, Aldo Cundari, and Silvano Sinigoi kindly provided the nodules investigated. Paolo Da Roit performed the microprobe analyses in Padova. Valeria Diella, Aldo Cundari and Silvano Sinigoi are gratefully thanked for their test microprobe analyses in Milan, Melbourne, and Modena, respectively. Enzo M. Piccirillo provided useful suggestions during the preparation of this work. G. Mezzacasa is thanked for drafting figures. Thanks are also due to the C.N.R. for financing the installation and maintenance of the electron microprobe laboratories in Milan and Modena. Financial support was also provided by Ministero della Pubblica Istruzione and by C.N.R. "Centro di Studio per i Problemi dell' Orogeno delle Alpi Orientali". The constructive comments of two anonymous referees significantly improved the manuscript.

## References

- Basso R, Dal Negro A, Della Giusta A, Rossi G (1979) Fe/Mg distribution in the olivines of ultramafic nodules from Assab (Ethiopia). *N Jb Min Mh* 5: 197–202
- Comin-Chiaramonti P, Della Giusta A, Flora O (1984) Crystal chemistry of four Mg–Fe–Al–Cr spinels from the Balmuccia peridotite (Western Italian Alps). *N Jb Min Abh* 150: 1–10
- Blessing RH, Coppens P, Becker P (1972) Computer analysis of step-scanned X-ray data. *J Appl Cryst* 7: 488–492
- Colby JW (1972) A computer program for quantitative electron microprobe analysis. Bell Telephone Laboratories Inc, Allentown, Pennsylvania.
- Comin-Chiaramonti P, Demarchi G, Girardi VAV, Princivalle F, Sinigoi S (1986) Evidence of mantle metasomatism and heterogeneity from peridotite inclusions of northeast Brazil and Paraguay. *Earth Planet Sci Letters* 77: 203–217
- Cundari A, Dal Negro A, Piccirillo EM, Della Giusta A, Secco L (1986) Intracrystalline relationships in olivine, orthopyroxene, clinopyroxene and spinel from a suite of spinel lherzolite xenoliths from Mt. Noorat, Victoria, Australia. *Contrib Mineral Petrol* 94: 523–532
- Dal Negro A, Carbonin S, Domeneghetti C, Molin GM, Cundari A, Piccirillo EM (1984) Crystal chemistry and evolution of the clinopyroxene in a suite of high pressure ultra-

- mafic nodules from the Newer Volcanics of Victoria, Australia. *Contrib Mineral Petrol* 86: 221–229
- Della Giusta A, Princivalle F, Carbonin S* (1986) Crystal chemistry of a suite of natural Cr-bearing spinels with  $0.15 \leq \text{Cr} \leq 1.07$ . *N Jb Min Abh* 155: 319–330
- Ellis DJ* (1976) High pressure cognate inclusions in the Newer Volcanics of Victoria. *Contrib Mineral Petrol* 58: 149–180
- Frey FA, Green DH* (1974) The mineralogy, geochemistry and origin of lherzolite inclusions in Victoria basanites. *Geochim Cosmochim Acta* 38: 1023–1059
- Hafner S* (1960) Metalloxyde mit Spinellstruktur. *Schw Mineral Petrol Mitt* 40: 208–240
- Hill RJ, Craig JR, Gibbs GV* (1979) Systematics of the spinel structure type. *Phys Chem Min* 4: 317–339
- Irving AJ* (1974) Pyroxene-rich ultramafic xenoliths in the Newer basalts of Victoria, Australia. *N Jb Min Abh* 120: 147–167
- Lindsley DH* (1976) The crystal chemistry and structure of oxide minerals as exemplified by the Fe-Ti oxides. In: *Rumble D III* (ed) *Oxide minerals*, Mineral Soc of America, Short Course Notes, Vol 3: 1–60
- O'Neill HStC, Navrotsky A* (1983) Simple spinels: crystallographic parameters, cation radii, lattice energies, and cation distribution. *Amer Mineral* 68: 181–194
- Ottonello G, Piccardo GB, Joron JL, Treuil M* (1978a) Evolution of the upper mantle under the Assab Region (Ethiopia): suggestions from petrology and geochemistry of tectonic ultramafic xenoliths and host basaltic lavas. *Geol Rund* 67-2: 547–575
- *Piccardo GB, Mazzucotelli A, Cimmino F* (1978b) Clinopyroxene-orthopyroxene major and rare earth element partitioning in spinel peridotite xenoliths from Assab (Ethiopia). *Geochim Cosmochim Acta* 42: 1817–1828
- (1980) Rare earth abundances and distribution in some spinel peridotite xenoliths from Assab (Ethiopia). *Geochim Cosmochim Acta* 44: 1885–1901
- Piccardo GB, Ottonello G* (1978) Partial melting effects on coexisting mineral compositions in upper mantle xenoliths from Assab (Ethiopia). *Rendiconti SIMP* 34: 499–526
- Princivalle F, Secco L* (1985) Crystal Structure Refinement of 13 Olivines in the Forsterite-Fayalite Series from Volcanic Rocks and Ultramafic Nodules. *Tschermaks Min Petr Mitt* 34: 105–115
- *Secco L, Demarchi G* (1989) Crystal chemistry of a clinopyroxene series of ultramafic xenoliths from North-Eastern Brazil. *Contrib Mineral Petrol* 101: 131–135
- Secco L* (1988) Crystal-chemistry of high-pressure clinopyroxene from spinel lherzolite nodules: Mts. Leura and Noorat Suites, Victoria, Australia. *Mineral Petrol* 39: 175–185
- Sinigoi S, Comin-Chiaramonti P, Demarchi G, Siena F* (1983) Differentiation of partial melts in the mantle: evidence from the Balmuccia Peridotite, Italy. *Contrib Mineral Petrol* 82: 351–359
- Urusov VS* (1983) Interaction of cation on octahedral and tetrahedral sites in simple minerals. *Phys Chem Min* 9: 1–5

Authors' addresses: Dr. *F. Princivalle*, Istituto di Mineralogia e Petrografia, Università di Trieste, Piazzale Europa 1, I-34127 Trieste, Italy. Prof. *A. Della Giusta* and Dr. *S. Carbonin*, Dipartimento di Mineralogia e Petrologia, Università di Padova, Corso Garibaldi 37, I-35100 Padova, Italy.